

# The breakdown of electrical insulation in a plane layer of insulating fluid by electrocapillary instability

By D. H. MICHAEL, M. E. O'NEILL

Department of Mathematics, University College London, Gower Street, W.C.1

AND J. C. ZUERCHER

Department of Electrical Engineering, Massachusetts Institute of Technology,  
Cambridge, Mass.

(Received 28 July 1970)

A theoretical and experimental study is made of the failure of electrical insulation in a layer of dielectric fluid filling a circular hole in a horizontal solid dielectric sheet. A potential difference is applied between conducting fluids which bound the fluid and solid dielectric layer above and below. It is observed that a critical potential difference is reached at which the fluid dielectric becomes statically unstable under the action of surface tension and normal electrical stresses at its interfaces. When this potential is reached the dielectric fluid insulation fails.

The critical potential difference is calculated by both an approximate and an exact theory. The approximate theory ignores the changes in the electrostatic field within the solid dielectric by allowing a charge distribution at the curved surface of the hole. Comparison with the results of an exact theory shows that such an approximation introduces only small errors in the calculated points of transition to instability.

It is shown that failure may take the form of a symmetric (sausage) mode of displacement, or an antisymmetric (kink) mode, depending on whether the radius of the hole is greater or less than approximately the depth of the layer respectively. The two forms of failure were indicated in the experiments, and the observed critical voltages are in good agreement with those predicted by the theory.

---

## 1. Introduction

In a recent paper Michael & O'Neill (1970) have given a discussion of plane waves on a horizontal layer of insulating fluid of infinite extent horizontally, and bounded vertically by semi-infinite conducting fluids which are at different electrostatic potentials. The problem, as discussed in that paper, was suggested by the work of Jayaratne & Mason (1964) on the effect of electric fields on the coalescence of water droplets with a water surface. It was shown that the marginal state between stable and unstable waves is a static one in which electrical and surface tensions are in balance at the interfaces.

Interfacial instability can be the cause of the failure of electrical insulation of a non-conducting fluid which is in contact with a fluid electrode. This phenomenon

has been demonstrated in the experimental work of Taylor & McEwan (1965) where, in fluid conductor/fluid insulator systems such as water/air and water/oil, instability precedes the electrical breakdown of the dielectric fluid. In this event jets of the conducting fluid formed by the growth of unstable disturbances precipitate the failure of the insulation. In a system such as mercury/air, however, electrical breakdown of the dielectric occurs at a potential difference lower than that for which interfacial instability arises.

Another form of instability has been demonstrated in an experimental and theoretical study by Atten & Moreau (1970), who have shown that when a non-conducting polar fluid is bounded by parallel plane solid electrodes, the dielectric fluid can become unstable through the injection of charge carriers. Such an instability leads to a cellular convection flow régime in the fluid.

In this paper we describe an experimental study which has recently been carried out by one of us (J. C. Zuercher) into the failure of insulation of a horizontal layer of insulating fluid bounded horizontally by a circular non-conducting wall. A potential difference is established between the upper and lower horizontal interfaces which are adjacent to fluid electrodes. The potential difference is raised until interfacial instability occurs, resulting in the failure of the fluid insulation. The paper also gives a mathematical analysis of the marginal state of incipient instability, using a model whose geometry matches that of Zuercher's experiments. It is shown theoretically, and indicated in the experiments, that the instability of the dielectric fluid may take different forms, depending on whether the radius of the wall is greater or less than approximately the depth of the layer. We have also determined theoretically the critical potential difference across the dielectric at which breakdown occurs, over a wide range of values of the ratio of wall radius to depth. The breakdown voltages obtained experimentally are compared with the theoretical values.

## 2. Preliminary discussion

The geometry of the experiments conducted by Zuercher is illustrated in figure 1. Conducting fluid occupies the space  $|z| > h$ , and the space  $|z| < h$  is filled with a layer of solid insulating material in which there is a circular hole containing a fluid insulator with the same density as the conducting fluid. The potential of the upper conductor is raised above that of the lower until breakdown of the fluid insulation occurs. The conditions of this experiment are closely related to those examined in Michael & O'Neill (1970), but the connexion requires further elucidation because the previous discussion analyses waves on an unbounded layer, whereas in this experiment the layer is bounded horizontally by the solid insulator.

The main results of the theory given previously are that the critical electrostatic fields at which plane waves of wave-number  $k$  become unstable, on an insulating layer of fluid of height  $2h$ , are given by

$$\kappa_1 E_0^2 = 4\pi kT \tanh kh, \quad (2.1)$$

or 
$$\kappa_1 E_0^2 = 4\pi kT \coth kh, \quad (2.2)$$

in Gaussian units. Here  $E_0$  denotes the applied electric field,  $T$  the surface tension and the dielectric fluid is assumed to have a dielectric constant  $\kappa_1$ . Equations, (2.1) and (2.2) apply to the symmetric ‘sausage’ modes, and the antisymmetric ‘kink’ modes respectively. Clearly for given  $k$  the lowest value of  $E_0$  at which this instability occurs will be that for a sausage mode. On an infinite layer of fluid all values of  $k$  are possible, but when the layer is bounded, the horizontal boundary conditions give rise to a discrete set of possible values of  $k$ .

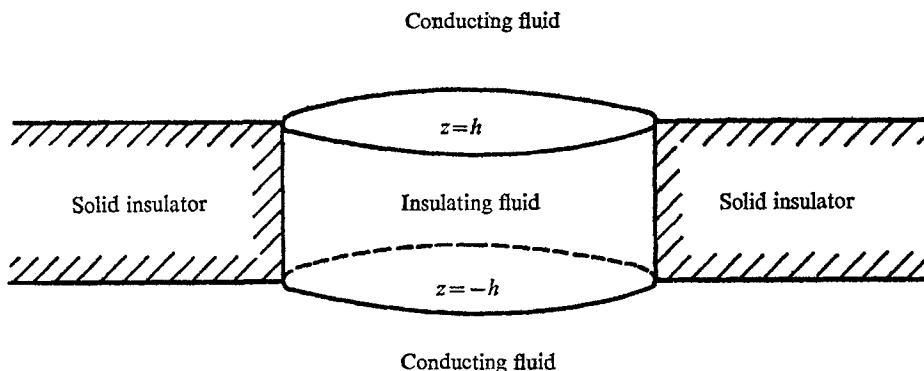


FIGURE 1. Schematic diagram of experiments.

In order to obtain results appropriate to the geometry of figure 1 it is desirable to write solutions in cylindrical polar co-ordinates  $(r, \theta, z)$ , where  $z$  is the vertical, and  $(r, \theta)$  polar co-ordinates from the centre of the circle in the horizontal plane. Let the upper and lower surfaces of the plane layer be  $z = \pm h$ , and the radius of the cavity  $r = R$ .

Let  $-E_0 \hat{z}$  be the applied electric field, and  $\chi$  a disturbance electrostatic potential when the insulating layer is slightly displaced. The conditions on  $\chi$  are that  $\nabla^2 \chi = 0$  and, at the top and bottom interfaces in contact with the conducting fluid, the potentials are unchanged. Thus if  $\zeta_1, \zeta_2$  represent the vertical displacements of the interfaces above and below respectively, in linearized theory  $\chi$  satisfies the condition  $\chi + E_0 \zeta_1 = 0$  at  $z = h$ , and  $\chi + E_0 \zeta_2 = 0$  at  $z = -h$ . It is significant that if  $\zeta$  is not zero at the edge of the surface interfaces at  $r = R$ , then  $\chi$  will be discontinuous at these points. To avoid this singularity it is necessary that  $\zeta_1 = \zeta_2 = 0$  at  $r = R$ .

A suitable solution of  $\nabla^2 \chi = 0$  for  $|z| < h$  and  $0 < r < R$  is

$$\chi = \sum_{i=1}^{\infty} \chi_{mi} \left\{ \frac{\sinh \alpha_{mi} z}{\cosh \alpha_{mi} z} \right\} e^{im\theta} J_m(\alpha_{mi} r), \tag{2.3}$$

in which  $m$  is an integer, and the summation is taken over the values of  $\alpha_{mi}$  for which  $J_m(\alpha_{mi} R) = 0$ . The form of  $\zeta$  consonant with (2.3) is

$$\zeta = \sum_{i=1}^{\infty} \zeta_{mi} J_m(\alpha_{mi} r) e^{im\theta}. \tag{2.4}$$

If we use the  $\sinh \alpha_{mi} z$  form we have the surface condition

$$E_0 \zeta_1 = -\chi_{mi} \sinh \alpha_{mi} h e^{im\theta} J_m(\alpha_{mi} r),$$

and  $\zeta_1 = -\zeta_2$  at corresponding points. Such a form of displacement will represent a transition of the sausage mode type. When  $\chi$  depends on  $\cosh \alpha_{mi} z$  the transition is such that  $\zeta_1 = \zeta_2$ , that is a kink mode. We may directly recover (2.1) and (2.2) so far as these equations are relevant, by applying the condition of continuity of stress at the interface, which is that, at each interface, the variation in surface tension is matched by the variation in electrical stress.

A solution of this form is not a mathematically exact solution to the problem, but it is instructive to examine in the first place its implications for the critical values of  $E_0$  for breakdown by instability. Subsequently we compare these results with an exact solution of the problem.

It is clear that whichever unstable mode occurs the critical value of  $E_0$  is to be determined by the lowest values of  $k = \alpha_{mi}$  which can occur. These are given by the solutions of the equation  $J_m(kR) = 0$ . For  $m = 0, 1, 2$ , we have

$$\left. \begin{aligned} m = 0: & \quad \alpha_{01} R = 2.405, & \alpha_{02} R = 5.520, \\ m = 1: & \quad \alpha_{11} R = 3.832, & \alpha_{12} R = 7.016, \\ m = 2: & \quad \alpha_{21} R = 5.135, & \alpha_{22} R = 8.417. \end{aligned} \right\} \quad (2.5)$$

However, the displacements of the interfaces must be such that the volume of insulating fluid is kept constant, assuming it to be incompressible. This condition introduces a constraint on the components of  $\zeta$  associated with  $m = 0$ , for the sausage mode only. In particular if the part of  $\zeta$  associated with  $m = 0$  is written as

$$\zeta_0 = \sum_{i=1}^{\infty} \zeta_{0i} J_0(\alpha_{0i} r),$$

then 
$$\int_0^R r \zeta_0 dr = - \sum_{i=1}^{\infty} \frac{\zeta_{0i}}{\alpha_{0i}} R J_1(\alpha_{0i} R) = 0,$$

the summation being taken over all the values of  $\alpha_{0i}$  for which  $J_0(\alpha_{0i} R) = 0$ .

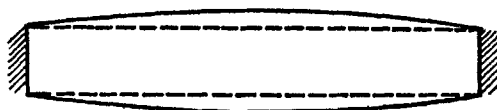
So far as a statical representation of the surface is concerned this does not introduce any constraint on the individual components. But it can be seen that the lowest possible value of  $E_0$  at which any mode can become unstable is that associated with the  $m = 0$  sausage mode for which  $i = 1$ . It might therefore be expected that such a mode would grow in time without proportional growth in the other modes associated with  $m = 0$ . This would clearly be precluded from continuity considerations, since this mode provides individually a contribution to the change in volume. This reasoning may clearly be generalized to yield the conclusion that sausage mode instability will not arise in any of the modes associated with  $m = 0$ , axisymmetric disturbances, since each such mode contributes to the change in volume. Such restrictions do not apply to the  $m = 0$  kink modes, or to the modes of either type when  $m \neq 0$ . Figure 2 shows the form of the surface displacements for the  $m = 0$ , and  $m = 1$  sausage and kink modes. From the preceding discussion instability can occur in the forms of figure 2 (b), (c) and (d) but not in figure 2 (a). Thus for the lowest breakdown voltages, we shall

expect the  $m = 1$  sausage mode and the  $m = 0$  kink mode to be significant. Substituting the values of  $\alpha_{mi}$  given by (2.5) in (2.1) and (2.2) we find

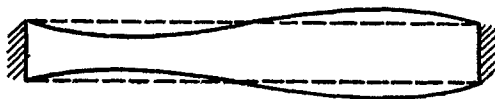
$$y_s = K_1 \frac{E_0^2 h}{4\pi T} = 3.832 \frac{h}{R} \tanh 3.832 \frac{h}{R}, \quad (2.6)$$

and

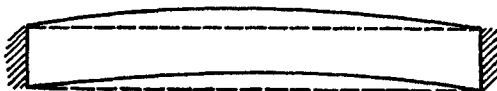
$$y_k = K_1 \frac{E_0^2 h}{4\pi T} = 2.405 \frac{h}{R} \coth 2.405 \frac{h}{R}, \quad (2.7)$$



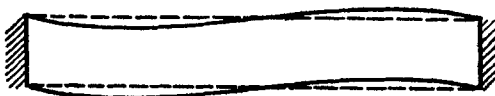
(a)



(b)



(c)



(d)

FIGURE 2. (a)  $m = 0$ , sausage mode; (b)  $m = 1$ , sausage mode; (c)  $m = 0$ , kink mode; (d)  $m = 1$ , kink mode.

for the lowest value of  $E_0$  in the sausage and kink modes respectively. These expressions as functions of  $(h/R)$  are plotted in figure 3. It is seen from figure 3 that when  $h/R < 0.367$  breakdown by instability should occur by a sausage mode with  $m = 1$  and for  $h/R > 0.367$  by a kink mode with  $m = 0$ .

The shortcomings of this form of analysis of the problem become evident when we examine the conditions on the fluid solid interface at  $r = R$ . Evidently from (2.4)  $\chi = 0$  at  $r = R$ , and since  $\chi = 0$  for  $z = \pm h$  and  $r > R$ , the solution for the potential inside the solid insulator is  $\chi = 0$  everywhere. This means that there is a discontinuity in the displacement vector, indicating the presence of charge at

the interface  $r = R$ . The behaviour of the insulating fluid observed in the experimental study, described in § 4, suggests that breakdown does not occur by charge passing along the walls of the circular hole. Thus it is necessary to modify the theory to allow for the continuity of the displacement vector at  $r = R$ . In the following section we give this form of solution.

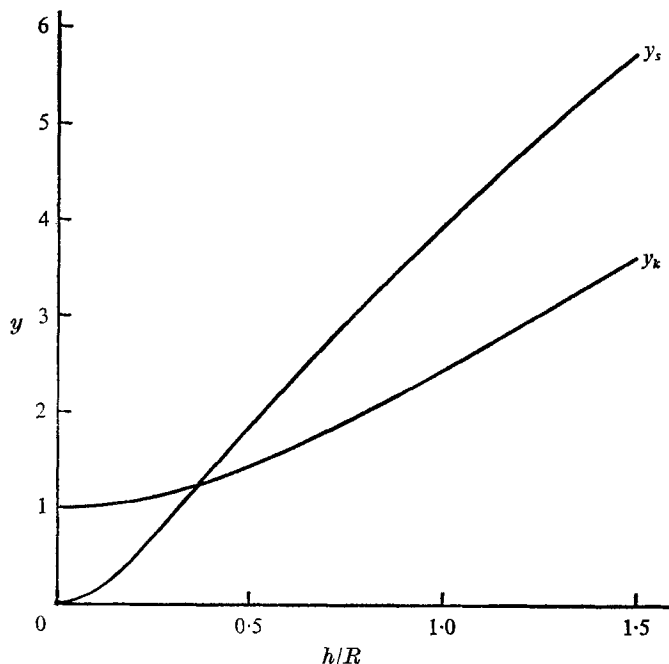


FIGURE 3. The functions  $y_s$  and  $y_k$ , defined by equations (2.6) and (2.7).

### 3. Exact mathematical theory

From the foregoing discussion it is clearly necessary to determine the perturbation electrostatic potential within the insulators in a way which allows the field in the region  $0 < r < R$  to be coupled with that in the region  $r > R$  to ensure zero charge on the liquid–solid interface.

Let  $\chi_1$  and  $\chi_2$  denote the perturbation electrostatic potentials in the liquid and solid insulators respectively. To allow for different dielectric constants in the solid and fluid insulators we now write

$$\chi_1 = \bar{\chi} + \chi_1^*, \quad \chi_2 = \bar{\chi} + \chi_2^*, \quad (3.1)$$

where  $\nabla^2 \chi_1^* = 0$  for  $0 < r < R$ ,  $|z| < h$  and  $\nabla^2 \chi_2^* = 0$  for  $r > R$ ,  $|z| < h$ . The function  $\bar{\chi}$  we choose so as to be continuous and differentiable at  $r = R$ ,  $|z| < h$  and to satisfy  $\nabla^2 \bar{\chi} = 0$  for all values of  $r$  and  $|z| < h$  together with the boundary conditions

$$\bar{\chi}(r, \pm h) = \begin{cases} -E_0 \zeta_1 & (0 < r < R), \\ 0 & (r > R), \end{cases} \quad (3.2)$$

$$\bar{\chi} \text{ bounded at } r = 0, \quad (3.4)$$

$$\bar{\chi} \rightarrow 0 \text{ as } r \rightarrow \infty, \quad (3.5)$$

for the antisymmetric kink mode disturbance. For the sausage mode the condition (3.2) is changed to

$$\bar{\chi}(r, \pm h) = \mp E_0 \zeta_1 \quad (0 < r < R). \tag{3.6}$$

It is clear that  $\bar{\chi}$  would represent the complete perturbation potential if the fluid and solid dielectrics have the same electrical properties. Using Hankel transform theory, it follows that the solution for a kink mode is

$$\bar{\chi} = -E_0 \sum_{m=0}^{\infty} e^{im\theta} \sum_{j=1}^{\infty} \zeta_{mj} \int_0^{\infty} \frac{k \cosh kz}{\cosh kh} F_m(\alpha_{mj}k) J_m(kr) dk, \tag{3.7}$$

where  $F_m(\alpha_{mj}, k) = \int_0^R J_m(\alpha_{mj}r) J_m(kr) r dr = \frac{\alpha_{mj}R}{k^2 - \alpha_{mj}^2} J_m(kR) J_{m-1}(\alpha_{mj}R).$  (3.8)

In the case of a sausage mode, the corresponding expression for  $\bar{\chi}$  is given by (3.7) with hyperbolic sines replacing hyperbolic cosines. The functions  $\chi_1^*$  and  $\chi_2^*$  for either a kink or sausage mode must satisfy the boundary conditions

$$\chi_1^*(r, \pm h) = 0, \quad (0 < r < R), \tag{3.9}$$

$$\chi_2^*(r, \pm h) = 0, \quad (r > R), \tag{3.10}$$

$$\chi_1^* = \chi_2^*, \quad (r = R, |z| < h), \tag{3.11}$$

$$\frac{\partial \chi_1^*}{\partial r} = \frac{\kappa_2}{\kappa_1} \frac{\partial \chi_2^*}{\partial r} - \frac{(\kappa_1 - \kappa_2)}{\kappa_1} \frac{\partial \bar{\chi}}{\partial r}, \quad (r = R, |z| < h), \tag{3.12}$$

$$\chi_1^* \text{ bounded at } r = 0, \quad \chi_2^* \rightarrow 0 \text{ as } r \rightarrow \infty, \tag{3.13}$$

where  $\kappa_1$  and  $\kappa_2$  denote the dielectric constants of the liquid and solid insulators respectively. For a kink mode, the solutions for  $\chi_1^*$  and  $\chi_2^*$  can be shown to be:

$$\chi_1^* = E_0 \sum_{m=0}^{\infty} e^{im\theta} \sum_{n=1}^{\infty} \sum_{j=1}^{\infty} A_{mnj} \zeta_{mj} I_m(\mu_n r/h) \cos(\mu_n z/h), \tag{3.14}$$

$$\chi_2^* = E_0 \sum_{m=0}^{\infty} e^{im\theta} \sum_{n=1}^{\infty} \sum_{j=1}^{\infty} B_{mnj} \zeta_{mj} K_m(\mu_n r/h) \cos(\mu_n z/h), \tag{3.15}$$

where  $\mu_n = (n - \frac{1}{2})\pi$  and

$$A_{mnj} = 2(-1)^n (\kappa_1 - \kappa_2) K_m(\mu_n R/h) P_{mnj}/h \Delta_{mn}, \tag{3.16}$$

$$B_{mnj} = A_{mnj} I_m(\mu_n R/h) / K_m(\mu_n R/h), \tag{3.17}$$

with  $P_{mnj} = \int_0^{\infty} k^2 (k^2 + \mu_n^2/h^2)^{-1} F_m(\alpha_{mj}, k) J'_m(kR) dk$  (3.18)

and  $\Delta_{mn} = \kappa_2 I_m(\mu_n R/h) K'_m(\mu_n R/h) - \kappa_1 I'_m(\mu_n R/h) K_m(\mu_n R/h).$  (3.19)

In the case of a sausage mode, equations (3.14) to (3.19) again hold, except that the dependence on  $z$  is  $\sin(\mu_n z/h)$  and  $\mu_n$  now denotes  $n\pi$ .

The critical electric field at which failure of the fluid insulation occurs by instability is determined from the normal stress condition at the interfaces between the conducting and dielectric fluids. It was shown in Michael & O'Neill

(1970) that for the unbounded fluid model the critical state is reached when the electrical and surface tension stresses at each interface just balance and this condition will not be altered by the presence of a rigid boundary  $r = R$  to the dielectric fluid. Accordingly electrical breakdown by fluid instability will occur when

$$T \left( \frac{\partial^2 \zeta}{\partial r^2} + \frac{1}{r} \frac{\partial \zeta}{\partial r} + \frac{1}{r^2} \frac{\partial^2 \zeta}{\partial \theta^2} \right) = \pm \frac{E_0}{4\pi\kappa_1} \frac{\partial \chi_1}{\partial z} \quad (0 < r < R), \tag{3.20}$$

where the + or - sign applies according as  $z = +h$  or  $z = -h$ . Now

$$\frac{\partial^2 \zeta}{\partial r^2} + \frac{1}{r} \frac{\partial \zeta}{\partial r} + \frac{1}{r^2} \frac{\partial^2 \zeta}{\partial \theta^2} = - \sum_{m=0}^{\infty} \left\{ \sum_{i=1}^{\infty} \alpha_{mi}^2 \zeta_{mi} J_m(\alpha_{mi} r) \right\} e^{im\theta}, \tag{3.21}$$

and for each  $m$  the functions  $J_m(\alpha_{mi} r)$ , ( $i = 1, 2, 3, \dots$ ) form a complete orthogonal set over the range  $0 < r < R$ . Thus within this range we may write

$$J_m(kr) = \frac{2}{R} \sum_{i=1}^{\infty} \frac{\alpha_{mi} J_m(kR) J_m(\alpha_{mi} r)}{(k^2 - \alpha_{mi}^2) J_{m-1}(\alpha_{mi} R)}, \tag{3.22}$$

$$I_m \left( \mu_n \frac{r}{h} \right) = - \frac{2}{R} \sum_{i=1}^{\infty} \frac{\alpha_{mi} I_m(\mu_n R/h) J_m(\alpha_{mi} r)}{(\mu_n^2/h^2 + \alpha_{mi}^2) J_{m-1}(\alpha_{mi} R)}. \tag{3.23}$$

By use of the equations (3.21) to (3.23) it follows that within the range  $0 < r < R$ , the derivatives of  $\bar{\chi}$  and  $\chi_1^*$  with respect to  $z$  on  $z = \pm h$  may be written in the form

$$\frac{\partial \bar{\chi}}{\partial z} = \mp E_0 \sum_{m=0}^{\infty} \left\{ \sum_{i=1}^{\infty} \sum_{j=1}^{\infty} \mathcal{C}_{mij} \zeta_{mj} J_m(\alpha_{mi} r) \right\} e^{im\theta}, \tag{3.24}$$

$$\frac{\partial \chi_1^*}{\partial z} = \mp E_0 \sum_{m=0}^{\infty} \left\{ \sum_{i=1}^{\infty} \sum_{j=1}^{\infty} \mathcal{D}_{mij} \zeta_{mj} J_m(\alpha_{mi} r) \right\} e^{im\theta}, \tag{3.25}$$

where the - or + sign is taken according as  $z = +h$  or  $z = -h$ . Because of the forms of the representations for  $\zeta$  and  $\chi_1$  it is clear that the terms on each side of (3.20) which involve  $m > 0$  vanish when  $r = 0$ , and since the expressions in (3.22) and (3.23) are valid when  $r = 0$  for  $m = 0$ , the conditions (3.20) will hold for  $0 < r < R$  provided that for each  $m$

$$4\pi\kappa_1 T \alpha_{mi}^2 \zeta_{mi} = E_0^2 \sum_{j=1}^{\infty} (\mathcal{C}_{mij} + \mathcal{D}_{mij}) \zeta_{mj}. \tag{3.26}$$

If we now write  $\lambda = 2\pi T/\kappa_1 E_0^2 h$ ,  $x = kh$ ,  $a = R/h$ ,  $Y_{mi} = \alpha_{mi} J_{m-1}(\alpha_{mi} R) \zeta_{mi}$ , and  $\xi_{mi} = \alpha_{mi} R$ , equation (3.26) reduces to

$$\lambda Y_{mi} = \sum_{j=1}^{\infty} (C_{mij} + D_{mij}) Y_{mj}, \tag{3.27}$$

where for a kink mode,

$$C_{mij} = \int_0^{\infty} \frac{x^2 \tanh x [J_m(ax)]^2 dx}{(x^2 - \xi_{mi}^2/a^2) (x^2 - \xi_{mj}^2/a^2)}, \tag{3.28}$$

$$D_{mij} = (\kappa_1 - \kappa_2) \sum_{n=1}^{\infty} \frac{I_m(\mu_n a) K_m(\mu_n a)}{\Delta_{mn} (\mu_n^2 + \xi_{mi}^2/a^2)} \times \int_0^{\infty} \left\{ \frac{\xi_{mj}^2/a^2}{(x^2 - \xi_{mj}^2/a^2)^2} + \frac{\mu_n^2}{(x^2 + \mu_n^2)^2} \right\} x [J_m(ax)]^2 dx, \tag{3.29}$$



with  $\Delta_{mn}$  as in (3.19). For a sausage mode  $C_{mij}$  is given by (3.28) with  $\tanh$  replaced by  $\coth$  and  $D_{mij}$  is given by (3.29) with  $\mu_n$  now denoting  $n\pi$ .

It therefore follows that for given values of  $T$ ,  $\kappa_1, \kappa_2$ ,  $h$  and  $a$ , the minimum value of  $E_0$  which produces instability in the dielectric fluid will be that value of  $E_0$  corresponding to the maximum of the set of all eigenvalues of the set of matrices  $C_{mij} + D_{mij}$  corresponding to  $m = 0, 1, 2, \dots$

In the case when the dielectric constants of both the fluid and solid dielectrics are the same  $D_{mij} = 0$ , and as  $C_{mij}$  is a real symmetric matrix for each  $m$ , all the values of  $\lambda$  satisfying (3.27) will be real.

Numerical evaluation of the eigenvalues of the matrix  $(C_{mij})$  has been carried out over a range of values of  $a$  from 0.1 to 8.0 for both kink and sausage modes when  $m = 1, 2$  and for the kink mode when  $m = 0$  also. It can be seen that the integrand of  $C_{mij}$  is never negative when  $i = j$  and so all diagonal elements are positive. However, when  $i \neq j$  the integrand is negative for  $\xi_{mi} < ax < \xi_{mj}$  ( $i < j$ ) and this has the effect of making all off-diagonal elements of  $(C_{mij})$  negative and much smaller in absolute magnitude than the diagonal elements. The numerical evaluations of  $C_{mij}$  have further shown that the elements of  $(C_{mij})$  decrease monotonically in absolute magnitude as  $i$  or  $j$  increases. In deciding a suitable choice of upper limit  $X$  of integration for the calculation of the elements of  $(C_{mij})$  we considered that with  $X = 200$  each  $C_{mij}$  could be determined to an accuracy of four decimal places since  $X^{-2}$  is an upper bound to the magnitude of the error in  $C_{mij}$  when the upper limit of integration is  $X$  provided that  $\xi_{mi}/a$  and  $\xi_{mj}/a$  are each no larger than about  $0.7X$ . The eigenvalues were evaluated by a successive approximation procedure in which the elements of the matrix and its eigenvalues were computed for  $1 < (i, j) < N$  with  $N$  first taking the value 2 and the procedure repeated with  $N$  increased by 1. When for a given value of  $a$ , the maximum eigenvalue  $\lambda_{\max}$  evaluated on two successive iterations agreed to at least three decimal places, it was assumed that this was the correct value of  $\lambda_{\max}$  to three decimal places. We found that for the range of values of  $a$  considered, the convergence of the iteration procedure was very rapid and to obtain  $\lambda_{\max}$  to the desired accuracy it was never necessary for  $N$  to exceed 5. Figure 4 shows the graphs of  $\lambda_{\max}$  for kink mode disturbances when  $m = 0, 1, 2$  and for sausage modes when  $m = 1, 2$ . It was pointed out in § 2 that the  $m = 0$  sausage mode is physically impossible.

Our numerical investigations thus suggest that for a given depth  $h$  of dielectric fluid, failure of the fluid insulation is associated with the instability of the  $m = 0$  kink mode for holes with radii less than about  $2.4h$  but for larger hole sizes it is the  $n = 1$  sausage mode which first becomes unstable as the potential difference between the conducting fluids is increased. These deductions are similar to those we conjectured in § 2, and in table 1, we display values of  $\lambda_{\max}$  for both the  $m = 0$  kink mode and the  $m = 1$  sausage mode which have been computed using the theory set out in this section where continuity of both the tangential component of the electric field and the normal component of the displacement vector at the interface between the fluid and solid dielectrics is taken into account. For comparison we also display values of  $\lambda^*$ , corresponding to  $\lambda_{\max}$ , if the condition of continuity of the normal component of displacement vector at  $r = R$  is relaxed

and the modified unbounded layers theory described in § 2 is applied. The expressions for  $\lambda^*$  may be deduced from equations (2.1) and (2.2) and are given by

$$\lambda^* = 2\pi T/E_0^2 \kappa_1 h = (a/2\xi_{01}) \tanh(\xi_{01}/a)$$

for the  $m = 0$  kink mode and

$$\lambda^* = 2\pi T/E_0^2 \kappa_1 h = (a/2\xi_{11}) \coth(\xi_{11}/a)$$

for the  $m = 1$  sausage mode.

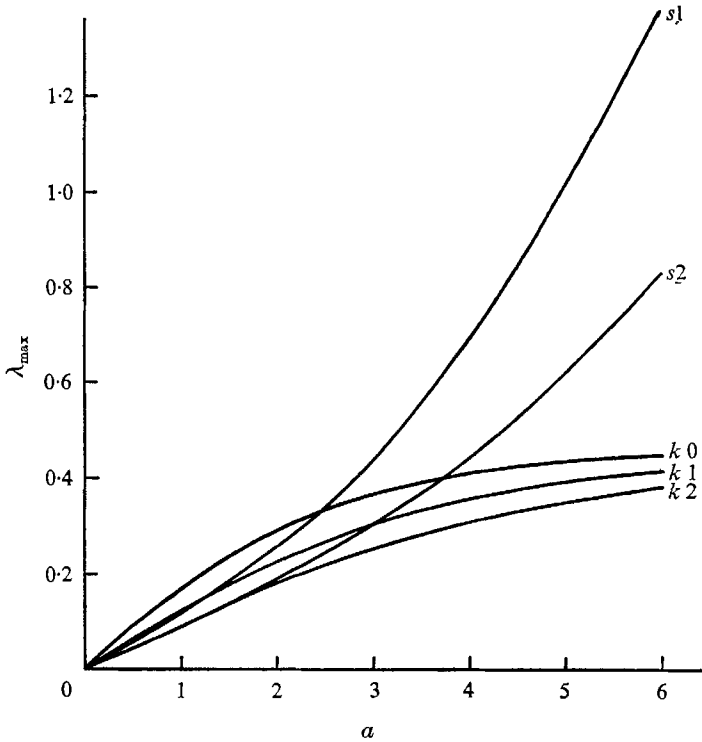


FIGURE 4. Value of  $\lambda_{\max}$  for kink modes when  $m = 0, 1, 2$  and sausage modes when  $m = 1, 2$  against  $a = R/h$ .

$a = R/h$	Kink mode $m = 0$		Sausage mode $m = 1$	
	$\lambda_{\max}$	$\lambda^*$	$\lambda_{\max}$	$\lambda^*$
0.10	0.018	0.021	0.012	0.013
0.125	0.023	0.026	0.015	0.016
0.25	0.045	0.052	0.030	0.033
0.5	0.090	0.104	0.061	0.065
1.0	0.173	0.205	0.122	0.131
2.0	0.295	0.347	0.262	0.273
4.0	0.408	0.447	0.694	0.702
6.0	0.450	0.475	1.382	1.388
8.0	0.469	0.485	2.339	2.343

TABLE 1

It is seen from table 1 that the critical values of  $\lambda$  obtained in the exact theory are well approximated by the original theory, especially for the very small and very large values of  $a$ . When  $a \gg 1$ , i.e.  $R \gg h$ , it might be expected that the two analyses would agree, since the boundary of the hole is at a large distance from the central part of it on the length scale  $h$  of the wavelength of the wave motion. As a measure of the discrepancy arising in the approximate theory we may take the level of surface charge density  $\sigma$  residing at  $r = R$  in that theory. For the kink mode, described by (2.4) we have

$$\chi = -E_0 \zeta_{mi} \frac{\cosh \alpha_{mi} z}{\cosh \alpha_{mi} h} e^{im\theta} J_m(\alpha_{mi} r), \quad (3.30)$$

where  $J_m(\alpha_{mi} R) = 0$ .

$$\text{Thus } \sigma = \frac{1}{4\pi\kappa_1} \left( \frac{\partial\chi}{\partial r} \right)_{r=R} = \frac{-E_0 \zeta_{mi}}{4\pi\kappa_1 h a} e^{im\theta} \zeta_{mi} J_{m+1}(\xi_{mi}) \frac{\cosh(\xi_{mi} Z/a)}{\cosh(\xi_{mi}/a)}, \quad (3.31)$$

where  $Z = z/h \sim 1$ . For modes with the lowest breakdown voltages  $\xi_{mi} \sim 1$ , and  $\sigma \rightarrow 0$  like  $1/a$  as  $a \rightarrow \infty$ . We might conclude from this that the error in  $\chi$  is  $O(1/a)$  at large  $a$ , and the error in  $\lambda^*$  is of the same order. The numerical results in table 1 are consistent with this. However, the error for both modes is appreciably less than  $1/a$  in proportion. It is also noticeable from the table that the value of  $\lambda^*$  for the  $m = 1$  sausage mode is a closer approximation to  $\lambda_{\max}$  than for the  $m = 0$  kink mode. This is perhaps because the total charge on the wall in all cases other than the  $m = 0$  kink mode, is in total zero.

Equations (3.30) and (3.31) also show why the approximate theory gives good agreement when  $a$  is small. In this case

$$\sigma \sim \frac{1}{a} \frac{\cosh(\xi_{mi} Z/a)}{\cosh(\xi_{mi}/a)} \sim \frac{1}{a} e^{-\xi_{mi}(1-|z|)/a},$$

the error being exponentially small, except near the surfaces  $Z = \pm 1$ . It is clear also from (3.30) that in this case the variable part of the electric field is confined to surface layers of thickness  $R \ll h$ .

The numerical calculations reported here appertain only to the case  $\kappa_1 = \kappa_2$ . In the experimental study described in the following section  $\kappa_2/\kappa_1 \approx 1.2$ . However, the present calculations show that the coupling between the two dielectric media only marginally affects the conditions at breakdown, so that a variation of  $\kappa_2/\kappa_1$  of this order would not be expected to give any substantial departures from the values of  $\lambda_{\max}$  obtained here.

#### 4. A short experimental study

A sketch of the apparatus is given in figure 5. In order to remove any effects due to gravity, the insulating fluid was chosen to be a mixture of Dow Corning 200 fluid (a low viscosity dimethylpolysiloxane) and  $\text{CCl}_4$ , having a density equal to that of tap water. This fluid was injected, using an eye dropper, into a waxed circular hole drilled into a  $\frac{1}{16}$  in. plexiglass sheet forming part of a frame of like material which in turn rested in a large pyrex dish filled with tap water. The water in the upper half of the frame was electrically isolated by the frame

walls from the water in the lower half of the frame and the rest of the container. The circular boundary of the hole was waxed to ensure that the insulating fluid would completely wet the wall, and so establish that there would be no surface displacement at the edge of the wall. This was verified especially in the case of the larger hole diameters, by noting the existence of a thin layer of insulating fluid (which was dyed red) at the boundary *after* instability had occurred. This would also indicate with some certainty that a breakdown due to free charge at the wall was not involved. The upper and lower electrodes were connected through a 3 kV d.c. source in series with an ammeter.

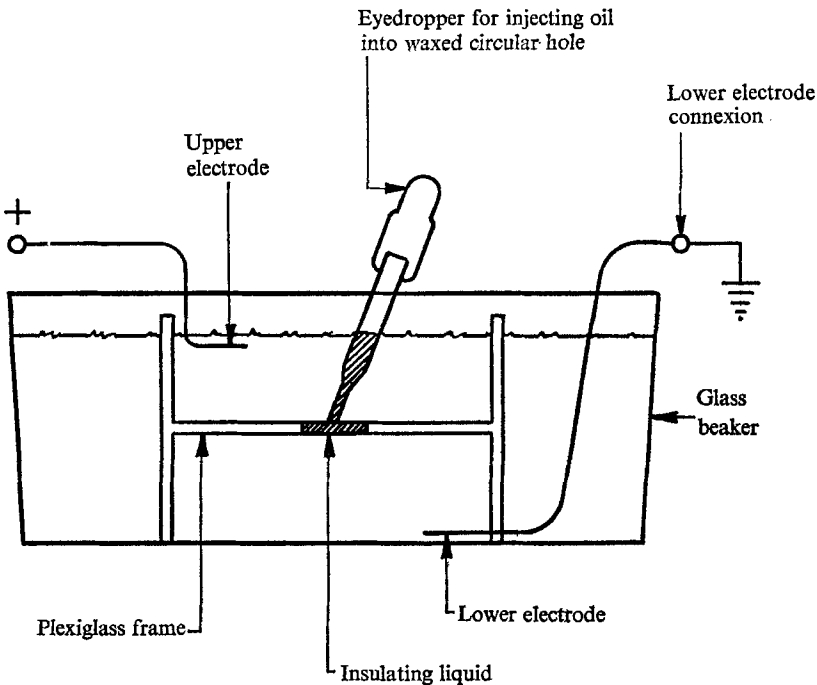


FIGURE 5. Schematic diagram of experimental apparatus.

As an increasing voltage was applied, the instability was marked by both a surge of current and either a puncturing of the insulating fluid for the larger hole diameters employed, or a violent ejection of the insulating fluid from the hole for the smaller hole diameters. The two forms of failure are illustrated in figure 6. The first form of instability is consistent with the wave-form of figure 2(b), a non-axisymmetric sausage mode, while the second form of breakdown corresponds to a kink mode such as is illustrated in figure 2(c). Figure 7 shows a plot of the experimental data, giving the critical potential difference  $V_c$  in kV against  $1/d$ , where  $d$  is the diameter of the hole in cm. The solid curves are derived from the theoretical solution of § 3 with  $\kappa_1 = \kappa_2$ ; thus with  $T$  in dynes/cm and  $h$  in cm, the theoretical value for  $V_c$  in kV is given by

$$V_c = 0.3(8\pi Th/\kappa_1 \lambda_{\max})^{\frac{1}{2}}.$$

The curves have been drawn to fit the experimental data by taking a value of  $T/\kappa_1 = 10.0$ . In some experiments, the insulating fluid was reused and in general it was found that the critical voltage was rather lower for cases when the same fluid had been used before. This accords with the observations of Taylor &

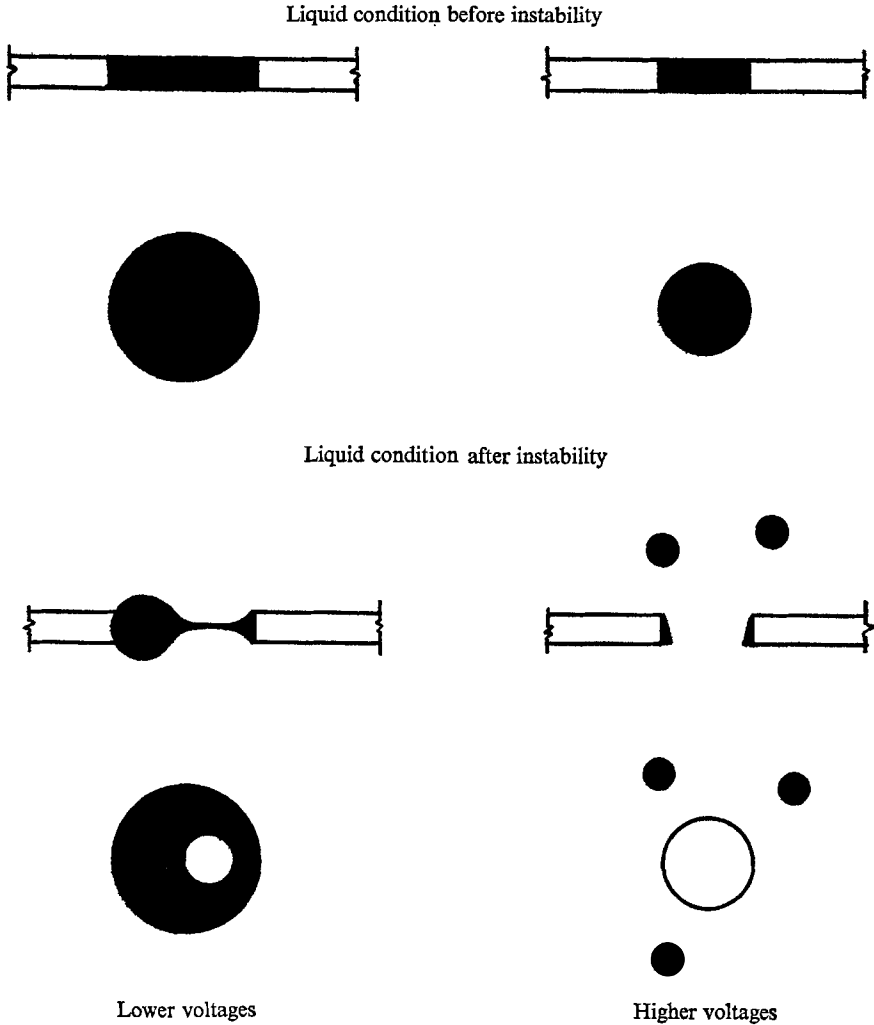


FIGURE 6. Illustration of the two forms of fluid instability.

McEwan (1965), that prestressed oil/water interfaces showed a lower resistance to instability.

There is reasonably good agreement between the theoretical curves and the experimental data; not only are the shapes of the curves, including the discontinuity in slope resulting from the transition of modes, reflected in the distribution of experimental data points, but in addition the observed difference in character of the instability for the larger or smaller hole diameters is consistent

with the theoretically predicted types of instability. Any discrepancies between the theoretical and experimental values of  $V_c$  are probably due to variations in the true thickness of the insulating fluid layer, which could be controlled only to within 20 %, and also to variations in the degree of its wetting of the plexiglass boundary.

A value of  $\kappa_1$  for the insulating fluid was obtained experimentally by a capacity measurement using a General Radio bridge. The value obtained was

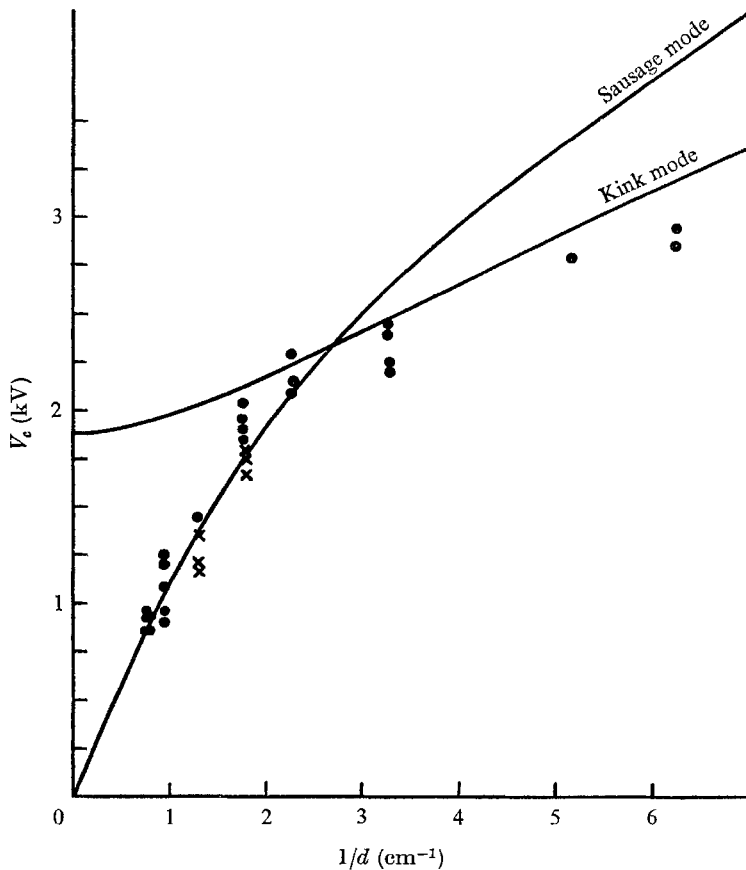


FIGURE 7. The abscissa measures the inverse hole diameter, and the ordinate the voltage at incipient instability for  $h = \frac{1}{32}$  in. The solid curves are theoretical plots, assuming  $T/\kappa_1 = 10$ , for the exact mathematical solution. ● indicates a measurement made with new liquid, whereas × indicates reused liquid.

$\kappa_1 = 2.59 \pm 0.15$ . This corresponds quite well with an arithmetic weighting by volume of the values 2.238 for  $\text{CCl}_4$  and 2.63 for the silicone oil, where the former is the book value for  $\text{CCl}_4$ , quoted from the *Handbook of Chemistry and Physics*, and the latter is a value obtained in the laboratory at M.I.T. The weighted value for the mixture based on these values is 2.57.

If we assume the value  $\kappa_1 = 2.6$  the theoretical curves given in figure 5 represent a value of  $T = 26$  dynes/cm. On this basis the mean value of  $T$  over

34 experimental points, using new fluid, was 26.66 with standard deviation 4.53. This is in general agreement with the value  $24 \pm 7$  dynes/cm for  $T$  determined by an independent direct measurement which involved balancing surface tension and gravitational forces.

The agreement obtained between theory and experiment confirms our view that the mechanism of collapse observed in these experiments was that of interfacial instability, and not the bulk dielectric breakdown mentioned in Taylor & McEwan (1965) nor unipolar injection instability discussed in Atten & Moreau (1970). A calculation based on current values given by Sazhin & Shuraev (1966) suggests that, in the notation of Atten & Moreau, the injection parameter  $C$  is at most  $10^{-2}$  and that  $M^2R < 10^6$ , thus confirming that these experiments were conducted in a region of stability, so far as unipolar convection is concerned.

We note in conclusion that the form of collapse observed here is sensitive to the ratio of hole diameter to hole depth in a way which is consistent with the interfacial instability mechanism, and that such behaviour would not be expected in either of the other two mechanisms.

Drs Michael and O'Neill wish to thank Miss S. M. Burrough for her assistance with the numerical work. Mr Zuercher wishes to thank Professor J. R. Melcher of the Electrical Engineering Department at M.I.T. for his encouragement of the experimental study, and also Dr E. P. Warren who assisted in overcoming some of the experimental problems.

## REFERENCES

- ATTEN, P. & MOREAU, R. 1970 *C. r. hebd. Séanc. Acad. Sci., Paris A* **270**, 415.  
JAYARATNE, O. W. & MASON, B. J. 1964 *Proc. Roy. Soc. A* **280**, 545.  
MICHAEL, D. H. & O'NEILL, M. E. 1970 *J. Fluid Mech.* **41**, 571.  
SAZHIN, B. I. & SHURAEV, V. P. 1966 *Sov. Electrochem.* **2**, 831.  
TAYLOR, G. I. & MCEWAN, A. D. 1965 *J. Fluid Mech.* **22**, 1.